ADVANCED FUNCTIONAL MATERIALS
www.afm-journal.de

Anisotropic Wettability of Biomimetic Micro/Nano Dual-Scale Inclined Cones Fabricated by Ferrofluid-Molding Method

*Chen-Yu Huang, Mei-Feng Lai, Wen-Lin Liu, and Zung-Hang Wei**

Learning from nature, a series of cone-shaped structures resembling trichomes of plants are fabricated by ferrofluid molding to understand the influence of geometry on wettability. Experimentally, ferrofluid microdroplets are generated under an external magnetic field, and their shape can be changed from right cones into oblique cones by tilting the external magnetic field. Followed by hard molds made with UV-curable tri(propylene glycol) diacrylate, polydimethylsiloxane microcones with different inclination angle (θ) are subsequently generated. Nickel thin film is deposited onto the microcones to form micro/nano dual-scale structures. The largest contact angle (CA) is obtained in nickel-deposited right cones (CA = 163.1° ± 2.5°). Anisotropic wettability is exhibited in oblique cones and the retention forces in the pin and release directions differ up to 12 μN (cones θ = 50°). As explained by a model as a function of the inclination angle of the cone structures, the contact and retention forces of droplet move in pin and release directions exhibit considerable differences. Results suggest the inclination of the trichomes assist the balance between repellency and retention of water in a direction-selective manner.

1. Introduction

Biological surfaces display intriguing wettability and adhesion properties have aroused interests in fundamental and biomimetic researches. Living organisms, such as Lotus leaf (*Nelumbo nucifera*),[1] and petals[2a,b] (**Figure 1**) with both micrometer and nanometer structures, would enable air to be entrapped and reduce the liquid–solid contact of the water droplets. Therefore, such surfaces have self-cleaning property or retain air films for respiration (e.g., *Salvinia spp.*).[3,4] Besides, the surface of the water-repellent species have been found to regulate the wettability and water transport. For instance, the capillary ratchet on the beaks of shorebirds guide the transport of droplets;[5] the flexible nano- and microscale structures overlapped on the wings of Morpho aega butterfly achieve directional adhesion of water droplet;[6] trichomes on the leaf surface are arranged with orientation to direct water droplets toward one end of the leaf to conserve water;[7] the wing surface of brown lacewing (Micromus tasmaniae) with microtrichia at different length-scale allow the insect to get through the wetted surfaces.[8]

The above-mentioned surface all contain microscale geometry with special arrangement or topographies to influence the surface property. Specifically, leaf surface contains various trichomes that for some incline at an acute angle to guide water[7] while others retain water on leaves to improved photosynthetic environment.[9] Inspired by the peculiar trichome structures, this study attempted to adopt cone-shaped structures to systematically understand how the inclination of the trichome influences the wettability of leaves.

Different strategies have been reported to obtain artificial microcone structures for the study of wetting property, including replica moulding,[2b,10] laser irradiation,[11–13] reactive ion etching (RIE),[14,15] and chemical deposition.[16] However, the above methods are complicated or not flexible enough to make microcones with tunable feature for our specific purpose. Previously, ferrofluid-molding method, which made use of ferrofluid as the master of the mother mold, has been demonstrated to fabricate microscale polymer arrays with controllable size.[17]

In this study, we utilized the similar technique and further, modified it for our particular purpose (**Figure 2**). In the experiment, microcone structures with different inclination angle were generated by adjusting the direction of external magnetic field applied to the ferrofluid. Nickel thin film was then deposited to give a nanoscale roughness layer. Wettability studies (contact angle, sliding angle) were analyzed, and the retention forces of droplet move against or along the orientation of cones were investigated.

2. Results and Discussion

To create cone-shaped structures resembling trichomes of plants, ferrofluid-molding method was adopted.[17] As shown in **Figure 3**a, the ferrofluid was divided into microdroplets due to magnetic hydrodynamic instability and were arranged by the magnetic disks to form a hexagonal pattern. As the external

C.-Y. Huang, W.-L. Liu, Prof. Z.-H. Wei
Department of Power Mechanical Engineering
National Tsing Hua University
Hsinchu City, Taiwan
E-mail: wei@pme.nthu.edu.tw
Prof. M.-F. Lai
Institute of NanoEngineering and MicroSystems
National Tsing Hua University
Hsinchu City, Taiwan

DOI: 10.1002/adfm.201500359

© 2015 WILEY-VCH Verlag GmbH & Co. KGaA, Weinheim

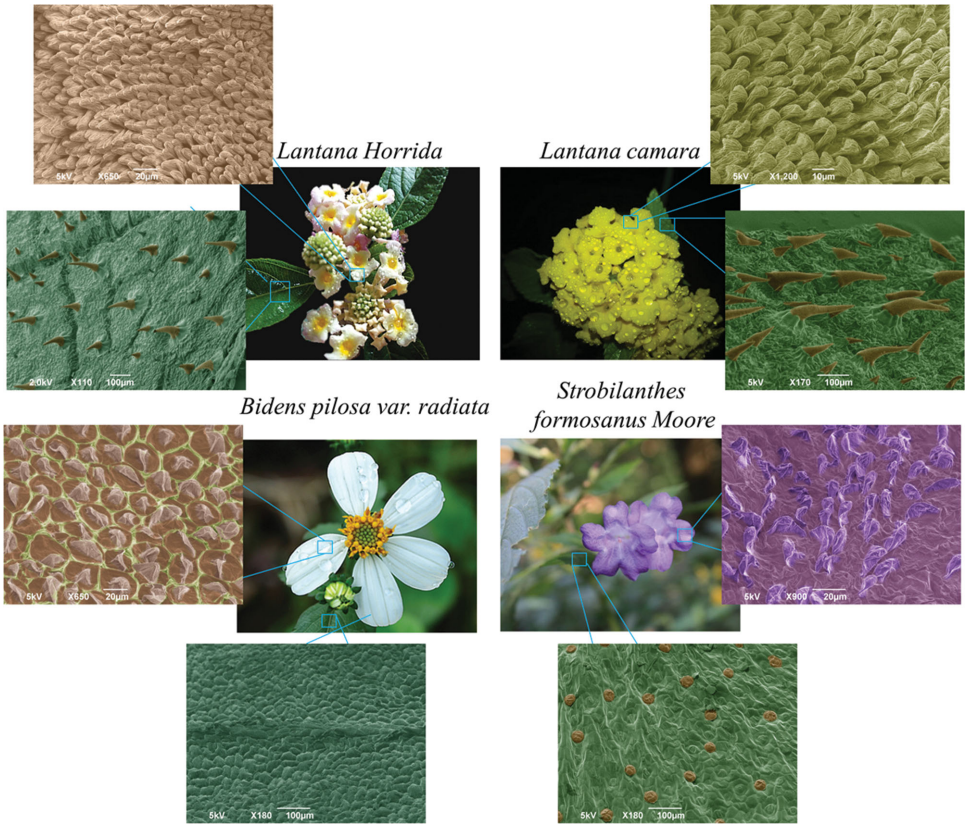

Figure 1. Colored SEM images of the plant. *Lantana Horrida*, *Lantana camara*, *Bidens pilosa var. radiata*, and *Strobilanthes formosanus Moore* were derived from National Tsing Hua University.

magnetic field (H) was tilted from its original longitudinal z-axis orientation into the transverse x–y plane, the ferrofluid droplets could follow the direction of the external magnetic field and be slanted (Video S1, Supporting Information). The ferrofluid droplets were then served as the master of the mother mold to fabricate cone-shaped polydimethylsiloxane (PDMS) (Figure 3b). Since the surface of trichomes contains various nanoscale structures that influence the wetting property, a nickel layer was further deposited onto the microstructures, as seen in **Figure 4**a–e. Right cones ($\theta = 90°$) and the cones with different inclination angle ($\theta = 0°$, 25°, 50°, 75°) have an apex angle of 31° (Figure 4f) with a base diameter of ≈120 µm, and are well distributed in a periodicity of 250 µm. Figure 4g is the magnification of a cone that shows hundreds of nanometers nickel structures. Figure 4h is an atomic force micrograph of a small surface region on the cone ($\theta = 0°$) that deposited with nickel, which show a mean roughness (Ra) of 99.5 nm and a root mean square (rms) of 130 nm.

To investigate the wetting property influenced by the inclination of cones, the static contact angle (CA) of water was observed by the sessile drop method to examine the wettability, as shown in **Figure 5**c,d. The intrinsic flat PDMS surface showed ordinary hydrophobicity with a CA of 102° ± 1.47°, while the nickel-deposited PDMS exhibited an increasing CA of 112° ± 2.45°. For those PDMS cones deposited with nickel showed higher CA than the original PDMS cones and the CA increase with respect

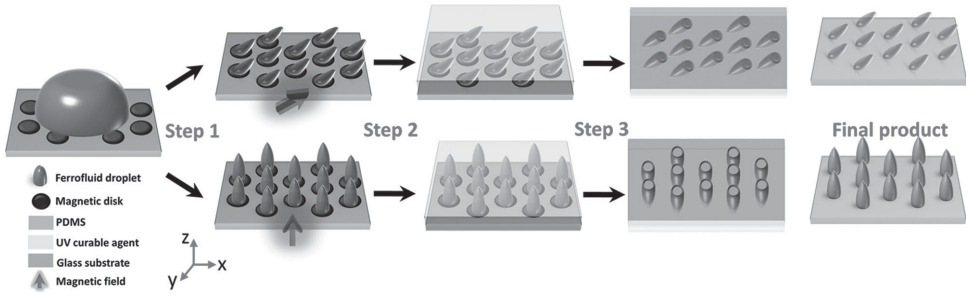

Figure 2. Schematic illustration of the fabrication process generating cone-shaped PDMS structures based on the ferrofluid-molding method. The magnetic field was applied in the out-of-plane direction (z-axis).

© 2015 WILEY-VCH Verlag GmbH & Co. KGaA, Weinheim

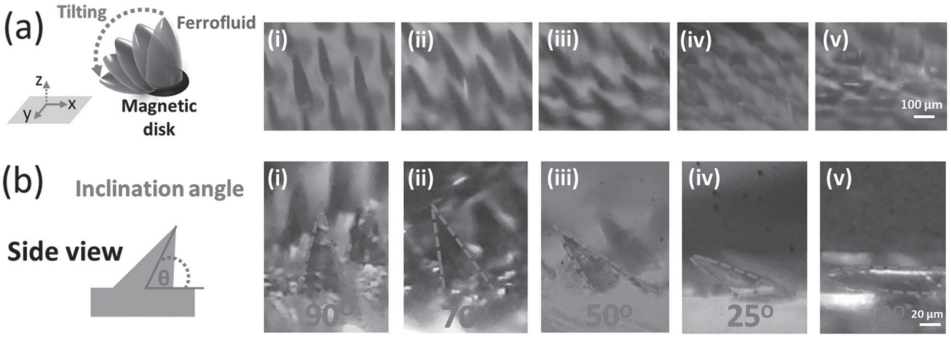

Figure 3. a) A series of snapshot during ferrofluid slanted by the tilting of out-of-plane magnetic field. b) The cone-shaped PDMS fabricated by ferrofluid-molding method. (i)–(v) The corresponding ferrofluid that served as the master of mother mold and the resulted PDMS cone structures. The inclination angle: the angle between the axis that passes through the center of the base and *x*-*y* plane.

to the inclination angle of the cones. Since air can be trapped in the micro/nanometer structures and beneath the droplet, a composite solid–liquid–air interface appeared and thus improved the superhydrophobicity (Figure 5a, picture show air pocket trapped between right cones).[18a,b] The microscale cone structures play an important role in reducing the contact area between solid and fluid at the macroscopic level, which leave spaces for air to retain; while the nanoscale nickel structures prevent liquid from filling the valleys between asperities. Therefore, the both levels of the hierarchy contribute to maintaining droplet in a stable Cassie state.[19] For the inclined asymmetric cones, the available space for air to be entrapped decrease, and the water–air interface become closer to the solid surface, as shown in Figure 5b. Besides, as the inclination angle is decreased, the contact area between droplet and cones increase and the solid–liquid–air interface become homogeneous; in other word, the three-phase contact line change from discontinuous characteristic to more quasi-continuous characteristic. Therefore, contact angles for the inclined cones become lower than that from right cones and decrease with the decrease of the inclination angle.[20] Figure 5e shows that a droplet bounce back into spherical shape from the surface of nickel-deposited right cones (CA = 163.1° ± 2.5°) and jump out quickly without retention (Video S2, Supporting Information). From the above results, the inclination of the trichomes play important role in helping retain and repel water, that is, to lift droplets above the surface but prevent it from jumping out easily, which would be beneficial for water reservation.

Figure 6 shows that the roll-off angle (*RA*, α) of droplet (volumes = 5, 7, 9 μL) moves along (release direction) or against (pin direction) the orientation of the nickel-deposited cone-shaped structures. For the asymmetric cones ($\theta = 25°$, 50°, 70°), the *RA* in the pin directions (α_1) are larger than those in the release directions (α_2) (Figure 6a), and the largest distinction between α_1 and α_2 occurred in cone-shaped PDMS ($\theta = 50°$). The incipient drop motion is the balance between the retention force (F_r), and the component of the gravitational force that parallel to the surface, which can be expressed as $F_r = \rho V g \sin\alpha$, where V is the volume of drop, ρ is the density, g is the gravitational acceleration. For cone-shaped PDMS ($\theta = 50°$), the retention force for 5–9 μL droplet in the pin direction is distinct from that along release direction, which are in the range of 32–40 and 19–28 μN, respectively (Figure 6d).

Further, to investigate how the liquid–solid contacts be changed by the inclination of microcones and affect the retention forces of droplet, **Figure 7** illustrate the advancing or receding contact lines of a droplet move in the pin direction and the release direction. According to the reports by Kawasaki[21]

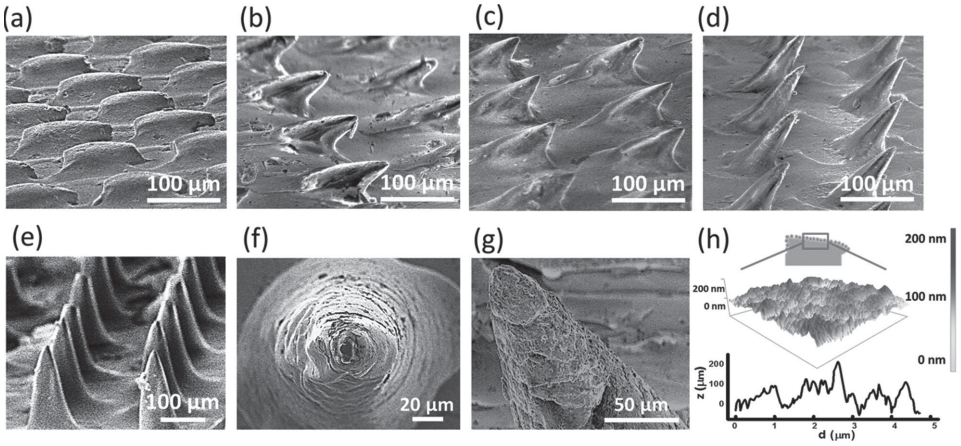

Figure 4. a–e) SEM images of the cone-shaped PDMS that deposited with nickel at different tilt angles (0°, 25°, 50°, 70°, and 90°). f) Top-view and g) the side view of high magnification SEM. h) 3D surface AFM image of a cone ($\theta = 0°$) that deposited with nickel. The scanning area is 5 μm × 5 μm. Height profile taken from cross-section is also shown.

© 2015 WILEY-VCH Verlag GmbH & Co. KGaA, Weinheim

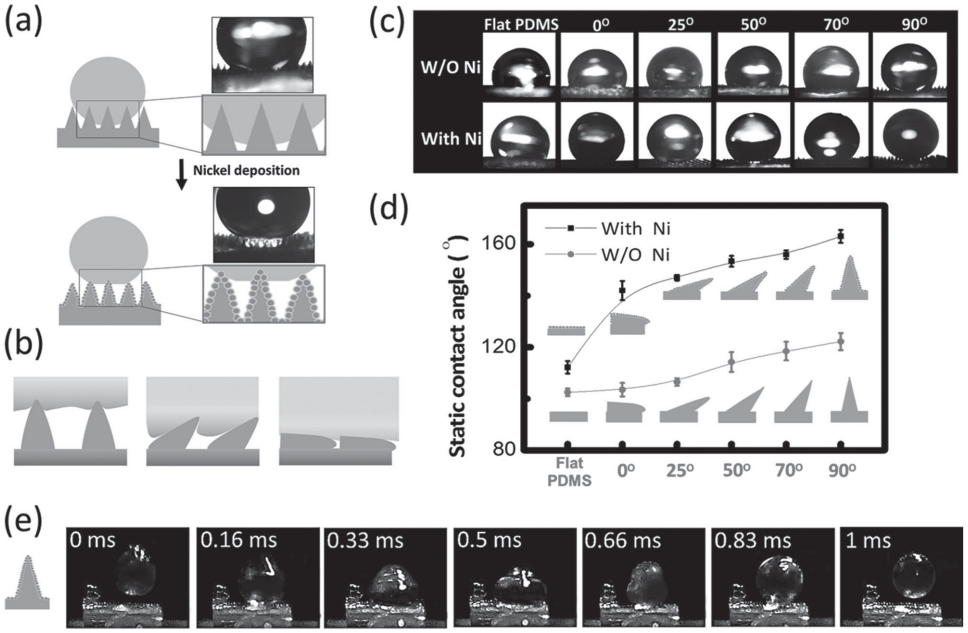

Figure 5. a) The illustration of static contact angle of a droplet on the as-prepared conical PDMS/ nickel-deposited conical PDMS. The inset photo shows clear air pockets formed in the cavities of nickel-deposited conical PDMS b) the illustration of the three-phase contact lines (solid–liquid–air) of the conical PDMS structures that inclined at different angles. As the inclination angle decreased, the three-phase contact lines change from discontinuous characteristics to more quasi-continuous characteristic. c,d) Static contact angle of the droplet on the as-prepared/nickel-deposited conical PDMS at different inclination angles ($\theta = 0°$, 25°, 50°, 70°, and 90°). e) High-speed images show that the droplet bounces and detaches from the superhydrophobic surface of nickel-deposited 90° conical PDMS.

and Furmidge,[22] a retention force resulting from the adhesion of the surface can be balanced by the gravity of a droplet that can be described as $f = w\,\gamma\,(\cos\theta r - \cos\theta a)$; where w is the contact width of a droplet, γ is the liquid surface tension. θr is the receding angle of the droplet; θa is the advancing angle of the droplet. Due to the complex solid–liquid–air contact lines of the inclined cone structures, we then combined the previously proposed models to approximate θa and θr,[10,23,24] which are related to the intrinsic contact angles θa_0 and θr_0 of the material, the tilt angle β and apex angle δ of the cone structures. For the inclined cones ($\theta = 25°$, 50°, and 70°), the movement of droplet along or against the orientation of cones result in different

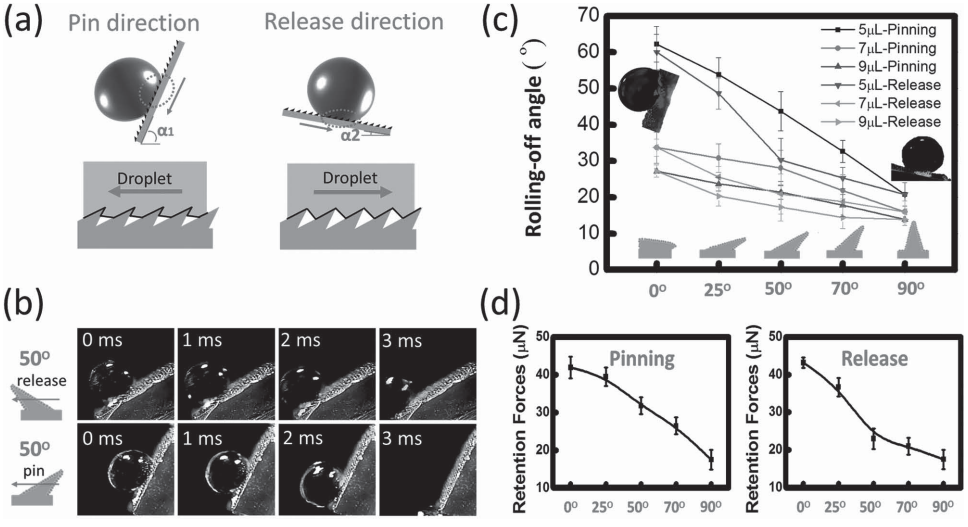

Figure 6. a) Illustration of a droplet moving along (release direction) or against (pin direction) inclined cone-shaped structures. The differences in the three-phase contact lines result in distinct roll-off angle ($\alpha 1 > \alpha 2$) for the two directions. b) The time sequences of snapshots of a droplet rolling off from the nickel- deposited cone-shaped structures at inclination angle of 50° in the release directions and pin directions. c) Rolling-off angle and d) the retention force of the droplet on the nickel-deposited cone-shaped structures at different inclination angle ($\theta = 0°$, 25°, 50°, 70°, and 90°) along release/pin direction.

© 2015 WILEY-VCH Verlag GmbH & Co. KGaA, Weinheim

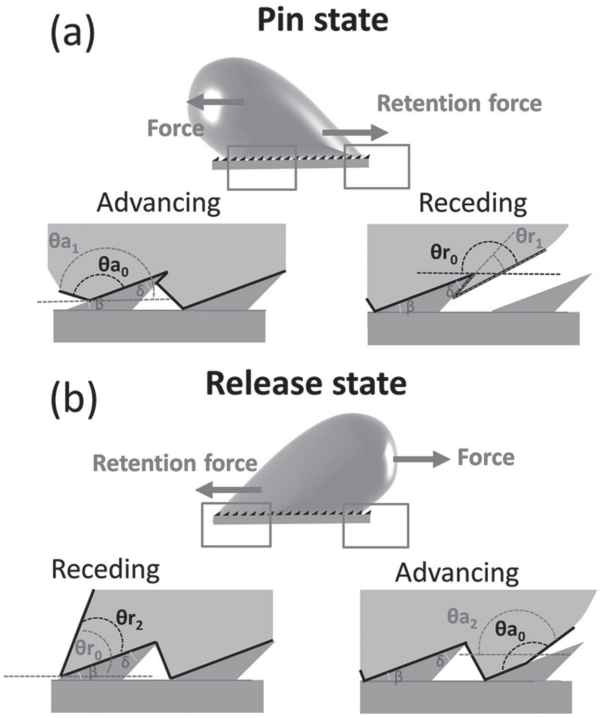

Figure 7. Schematics of drop on inclined cone-shaped structures and the enlarged view of advancing and receding edges. The contact between the drop and elements when the drop is moved a) in the release and b) the pin directions is illustrated. The contact angles θ_a and θ_r between the advancing and receding menisci and the substrate axis are functions of the intrinsic contact angles θa_0 and θr_0 of material, the tilt angle β, and apex angle δ. At the pin state, the advancing angle $\theta a_1 = \theta a_0 - \beta$ and receding angle $\theta r_1 = 180° - \theta r_0 - (\beta + \delta)$. At the release state, the moving of droplet follow the orientation of the cones, and the three-phase contact line is changed slightly with the advancing angle $\theta a_2 = \theta a_0 - \beta$ and receding angle $\theta r_2 = \theta r_0 + \beta$. Note that the substrate constrains θa and θr to be between 0° and 180°.

three-phase contact lines. In the pin direction (Figure 7a), the advancing angle $\theta a_1 = \theta a_0 - \beta$ and receding angle $\theta r_1 = 180° - \theta r_0 - (\beta + \delta)$. While at the release state (Figure 7b), the droplet with advancing angle $\theta a_2 = \theta a_0 - \beta$ and receding angle $\theta r_2 = \theta r_0 + \beta$. The intrinsic advancing angle (θa_0) and receding angle of nickel-deposited flat PDMS (θr_0) are 116° and 55°, respectively. For the inclined cone-shaped structures with inclination angle (θ) of 25°, 50°, and 70°, the respective tilted up angle (β) are 15°, 30°, 55° and apex angle δ is 31°. The retention force, f in either direction ($f_{\text{pin,release}}$) can be further described as

$$f_{\text{pin,release}} \sim 2w_{\text{pin,release}}\gamma\left[\sin\left(\frac{\theta_{\alpha 0}+\theta_{r0}}{2}-\varphi_{\text{pin,release}}\right)\sin\left(\frac{\theta_{\alpha 0}-\theta_{r0}}{2}-\tau_{\text{pin,release}}\right)\right] \quad (1)$$

where $\varphi_{\text{pin}} = (180° - \delta)/2$; $\varphi_{\text{release}} = 0$ and $\tau_{\text{pin}} = \beta - (180° - \delta))/2$; $\tau_{\text{release}} = \beta$; $w = 2\pi R\lambda$, where R is the contact radii of a drop, λ is linear solid fraction which proportion related to the cone section diameters (Max = 120 μm, Min = 9 μm). We considered the maximum (w_{min}) and the minimum contact width (w_{min}) to occur, respectively, in the pin and the release direction and estimated $w_{\text{max}}/w_{\text{min}}$ in **Table 1**. The cone-shaped PDMS ($\theta = 50°$) has maximum $w_{\text{max}}/w_{\text{min}}$ value of 13.3, and the $f_{\text{pin}}/f_{\text{release}}$ could be up to 146.9. The difference in the water contact lines at two directions cause the change of the fraction of solid–liquid–air interface and retention force. The largest $w_{\text{max}}/w_{\text{min}}$ occur in cone-shaped PDMS (θ = 50°) is coordinated with the result from Figure 6 and imply that the inclination of the cone help the retention of water droplet in a direction-selective manner.

Table 1. Estimated contact width (w) and retention force (f) of cone-shaped structures.

θ	Tilt angle β	$w_{\text{pin}}/w_{\text{release}}$	$f_{\text{pin}}/f_{\text{release}}$
25°	15° ± 1.03°		1.37–18.31
50°	30.3° ± 2.07°	1–13.3[a)]	11.05–146.96
70°	55.4° ± 2.13°		2.67–35.54

[a)] Maximum and minimum cone section diameters are 120 and 9 μm.

The trichomes not only maintain droplets staying in Cassie state to minimize the wetted area of immersed surfaces but also guide the droplets for water reservation. As proposed previously, water-repellent plants like Lady's Mantle (*Alchemilla vulgaris L.*) and Lupin (*Lupinus spp.*) contain trichomes to create solid–liquid–air interfaces to slow down the water droplet and to guide droplet to fallout near the plant roots.[7,25] For this reason, the inclination of plant trichomes could be extremely useful for water/air management. Such special arrangement in the present trichome systems of leaves may attribute to the natural selection for better water management.

In this research, the ferrofluid-molding method enabled us to fabricate microcones with different inclination angle and was demonstrated to be potential for systemically investigating natural phenomena. Previously, straight silicon[26] or PDMS pillars[27] have been deflected to form slanted pillars by oblique metal deposition. By utilizing our proposed method, arrays of uniform asymmetric structures that consist of more complex geometry (oblique cones) can be generated, and the inclination angle of microcones can be tuned by simply adjusting the magnetic field applied to the ferrofluid. This method offers new opportunities to design asymmetric structures for future applications.

3. Conclusion

Learning from nature, we have been inspired to construct a series of cone-shaped structures for studying the wettability influenced by the inclination of trichomes on leaf surface. Micro/nano dual-scale PDMS cones with different inclination angle were fabricated via ferrofluid-molding method, and their wettability have been analyzed. The retention forces of droplet exhibited ≈12 μN differences between the movement that along or against the orientation of cones (θ = 50°). The contact width and retention force as droplet move in pin and release directions were investigated. The results suggested that the inclination of the cone-shaped microstructures assisted the balance between the repellency and retention of water in a direction-selective manner, which indicated the inclination of leaf trichomes is optimized through natural selection.

© 2015 WILEY-VCH Verlag GmbH & Co. KGaA, Weinheim

4. Experimental Section

Resources of Flower and Leaves: The flower and leaves of *Lantana Horrida*, *Lantana camara*, *Bidens pilosa var. radiata*, *Strobilanthes formosanus Moore* were collected from from the campus of National Tsing Hua University.

Fabrication of the Cone-Shaped PDMS Structures: Fabrication processes based on ferrofluid-molding method are shown in Figure 2. Initially, 3 μL of water-based ferrofluid droplet containing 10 nm magnetic nanoparticles was dropped on the glass that was deposited with the hexagonal arrays of magnetic disks. The diameter of each disk and center-to-center distance between neighboring magnetic disks was 150 and 250 μm, respectively. A cylindrical permanent magnet was placed below the glass substrate to apply an out-of-plane magnetic field H and triggered magnetic hydrodynamic instability of ferrofluid. The large cylindrical permanent magnet with a diameter of 50 mm and a height of 6 mm provided relatively homogeneous local magnetic field to the glass substrate. The ferrofluid would divide into microdroplets to form hexagonal patterns to minimize the system energy and attracted/pinned by the magnetic disks (Figure 2, step 1). The magnetic field H was tilted out from the original z-axis orientation into the x-y plane by rotating the cylindrical permanent magnet, and the shape of the ferrofluid could be changed from right cones into oblique cones. UV curable agent, tri(propylene glycol) diacrylate (TPGDA, Chembridge International Corp.) was used to replicate the negative structure of the microdroplets and generated a mold with cavities (Figure 2, step 2). Polytetrafluoroethylene (PTFE or Teflon, DuPont Corp.) was then spin coated onto the surface of the mold to lower surface energy. Thereafter, the prepolymer of polydimethylsiloxane (PDMS, SYLGARD 184, Dow Corning Corp.) was diluted with silicon oil in the proportions 4:1 (v:v), put into a vacuum chamber to remove the entrapped air bubbles, and then be poured to cover the mold made by UV curable agent to fill the cavities (Figure 2, step 3). The diluted PDMS was used instead of the pure PDMS material was due to its flexibility for maintaining the high-aspect-ratio microstructures.[28] After heated at 90 °C for 1 h, the PDMS surface was peeled off carefully, and slowly separated directionally from the surface along the orientation of the cone-shaped structures (Figure 2, Final product).

Nano-Scale Roughness Created by Electron-Beam Evaporation: About 300 nm of nickel thin film was deposited by electron-beam evaporation system (FU-PEB-500, Fulintec), which enabled a layer of nanoscale polycrystalline structures to be formed on the PDMS surface. By means of the van der Waals force between the nanocrystalline and the PDMS surface, nickel metal thin film could be stabilized on the PDMS surface, and such metal crystalline structures were hard to be washed away by water and possessed long-term durability as contact with water. Therefore, desired polymer cone-shaped structures with fine nanometric structures were achieved effectively. The stability of the superhydrophobicity after storage in air for various time intervals was also investigated and remains constant after storage about 2 months in the air, showing the long-term stability of the fabricated surface.

Contact Angle (CA) Measurement: The static contact angles were tested by the sessile drop method that was performed in air at ambient temperature, and the value reported was the average of 20 measurements from the same sample. To exam the anisotropy of the artificial surface, roll-off angle was measured by tilting the stage (tilt rate = 1.7° s^{-1}) until incipient motion of the droplet was detected and the drop volumes were 5, 7, 9 μL. The roll-off angles of the drop's move along or against the orientation of the cone-shaped structures were recorded. The dynamic process of the drop shedding off from the surface was captured by a high-speed camera (Nikon).

Characterization: Surface morphology were analyzed using atomic force microscopy (AFM, Dimension 3100 Scanning Probe Microscope (D3100), Veeco Inc.) in tapping mode under ambient conditions using silicon cantilevers (spring constant 2.8 N m^{-1}) and the image was processed by Digital Instruments Nanoscope III. The microstructures of the surface were observed by Scanning Electron Microscopy (SEM, JSM-6390, JEOL Ltd.), under an accelerating voltage of 3–5 kV. In addition, sample stages were adjusted by tilt angles 45° for 3D feature investigation. Cone-shaped PDMS structures were visualized using an Olympus optical microscope.

Supporting Information

Supporting Information is available from the Wiley Online Library or from the author.

Acknowledgements

This work was supported in part by the Ministry of Science and Technology, Taiwan (TW) under Grant Nos. NSC 102-2112-M-007-012-MY3, and NSC 103-2221-E-007-017-MY2.

Received: January 28, 2015
Revised: March 5, 2015
Published online: March 25, 2015

[1] R. N. Wenzel, *Ind. Eng. Chem.* **1936**, *28*, 988.
[2] a) B. Bhushan, E. K. Her, *Langmuir* **2010**, *26*, 8207; b) A. J. W. Schulte, D. M. Droste, K. Koch, W. Barthlott, *Beilstein J. Nanotechnol.* **2011**, *2*, 228.
[3] W. Barthlott, T. Schimme, S. Wiersch, K. Koch, M. Brede, M. Barczewski, S. Walheim, A. Weis, A. Kaltenmaier, A. Leder, H. F. Bohn, *Adv. Mater.* **2010**, *22*, 2325.
[4] Z. Cerman, B. F. Striffler, W. Barthlott, in *Functional Surfaces in Biology* (Ed: S. N. Gorb), Springer, The Netherlands **2009**, Vol. *1*, Ch. 6.
[5] M. Prakash, D. Quéré, J. W. M. Bush, *Science* **2008**, *320*, 931.
[6] Y. Zheng, X. Gao, L. Jiang, *Soft Matter* **2007**, *3*, 178.
[7] N. J. Shirtcliffe, G. McHale, M. I. Newton, *Langmuir* **2009**, *25*, 14121.
[8] J. A. Watson, B. W. Cribb, H. M. Hu, G. S. Watson, *Biophys J.* **2011**, *100*, 1149.
[9] W. K. Smith, T. M. McClean, *Am. J. Bot.* **1989**, *76*, 465.
[10] P. Guo, Y. Zheng, C. Liu, J. Ju, L. Jiang, *Soft Matter* **2012**, *8*, 1770.
[11] J. Shao, Y. Ding, W. Wang, X. Mei, H. Zhai, H. Tian, X. Li, B. Liu, *Small* **2014**, *10*, 2595.
[12] E. Stratakis, A. Ranella, C. Fotakis, *Biomicrofluidics* **2011**, *5*, 013411.
[13] B. Wu, M. Zhou, J. Li, X. Ye, G. Li, L. Cai, *Appl. Surf. Sci.* **2009**, *256*, 61.
[14] X. M. Zhang, J. H. Zhang, Z. Y. Ren, X. Li, X. Zhang, D. F. Zhu, T. Q. Wang, T. Tian, B. Yang, *Langmuir* **2009**, *25*, 7375.
[15] J. Linders, H. Niedrig, H. Koch, *Nucl. Instrum. Methods Phys. Res.* **1986**, *13*, 309.
[16] X. Yao, Q. Chen, L. Xu, Q. Li, Y. Song, X. Gao, D. Quere, L. Jiang, *Adv. Funct. Mater.* **2010**, *20*, 656.
[17] C. P. Lee, Y. H. Chen, M. F. Lai, *Microfluid. Nanofluid.* **2014**, *16*, 179.
[18] a) A. B. D. Cassie, S. Baxter, *Trans. Faraday Soc.* **1944**, *40*, 546; b) B. Bhushan, Y. C. Jung, *J. Phys. Condens. Matter* **2008**, *20*, 225010.
[19] Y. Su, B. Ji, K. Zhang, H. Gao, Y. Huang, K. Hwang, *Langmuir* **2010**, *26*, 4984.

© 2015 WILEY-VCH Verlag GmbH & Co. KGaA, Weinheim

[20] M. Nosonovsky, B. Bhushan, *Microsyst. Technol.* **2006**, *12*, 273.
[21] K. Kawasaki, *J. Colloid Sci.* **1960**, *15*, 402.
[22] C. G. L. Furmidge, *J. Colloid Sci.* **1962**, *17*, 309.
[23] N. A. Malvadkar, M. J. Hancock, K. Sekeroglu, W. J. Dressick, M. C. Demirel, *Nat. Mater.* **2010**, *9*, 1023.
[24] C. W. Extrand, *Langmuir* **2007**, *23*, 1867.
[25] A. Otten, S. Herminghaus, *Langmuir* **2004**, *20*, 2405.
[26] K. H. Chu, R. Xiao, E. N. Wang, *Nat. Mater.* **2010**, *9*, 413.
[27] X. M. Yang, Z. W. Zhong, E. Q. Li, Z. H. Wang, W. Xu, S. T. Thoroddsencd, X. X. Zhang, *Soft Matter* **2013**, *9*, 11113.
[28] H. Kang, J. Lee, J. Park, H. H. Lee, *Nanotechnology* **2006**, *17*, 197.

© 2015 WILEY-VCH Verlag GmbH & Co. KGaA, Weinheim